

Electrical transport characteristics of ruthenium/n-InP Schottky diodes from current-voltage-temperature (I-V-T) measurements

V. JANARDHANAM*, A. ASHOK KUMAR, V. RAJAGOPAL REDDY, P. NARASIMHA REDDY
Department of Physics, Sri Venkateswara University, Tirupati, Andhra Pradesh, INDIA-517 502

The current-voltage (I-V) characteristics of Ru/n-InP Schottky diodes were measured in the temperature range 200 – 400 K. The I-V curves fitted by the equation based on thermionic emission theory has revealed decrease of zero-bias barrier height and increase of ideality factor with decreasing temperature. This behavior has been interpreted by the assumption of Gaussian distribution of barrier heights due to barrier inhomogeneities that prevail at the metal-semiconductor interface. $A \Phi_{b0}$ versus $q/2kT$ plot was drawn to obtain evidence of Gaussian distribution of barrier heights yielded values of $\Phi_{b0} = 0.79$ eV for mean barrier height and $\sigma_0 = 0.122$ eV for standard deviation at zero-bias. The modified Richardson plot gives $\Phi_{b0}(T=0) = 0.81$ eV and $A^{**} = 5.73$ A K⁻² cm⁻². It can be concluded that the temperature dependence of I-V characteristics of the Schottky barrier on n-InP can be successfully explained on the basis of TE mechanism with Gaussian distribution of the barrier heights.

(Received September 1, 2008; accepted September 26, 2008)

Keywords: Schottky diodes, Indium phosphide, I-V characteristics, Barrier height, Ideality Factor, Series resistance

1. Introduction

Indium phosphide (InP) is an attractive III-V compound semiconductor for high speed semiconductor devices such as metal-semiconductor field-effect transistors (MESFETs), optoelectronic applications and high-speed electronic devices due to its direct transition bandgap and high electron mobility, both of which are very important in these devices [1-3]. However, a serious drawback of InP is the Schottky barrier diodes (SBDs) with low barrier height (BH) and have found applications in devices operating at cryogenic temperatures as infrared detectors and sensors in thermal imaging [4, 5]. Schottky junctions are one of the most widely used rectifying junctions in the electronics industry [6-9]. Metal-semiconductor (MS) structures are important research tools in the characterization of new semiconductor materials and at the same time, the fabrication of these structures plays a crucial role in constructing some useful devices in technology [2,6,9,10]. Therefore, there has been considerable interest in the study of the Schottky contact formation for the characterization of semiconductor devices.

Analysis of the current-voltage (I-V) characteristics of the Schottky diodes obtained only at room temperature does not give detailed information about the charge transport process and about the nature of the barrier formed at the metal-semiconductor interface. In fact it neglects many possible effects that cause non-ideality in the I-V characteristics of the diode and reduce the barrier height. The temperature dependence of the I-V characteristics gives a better understanding of the

conduction mechanism and allows one to understand different aspects that shed light on the validity of various processes involved [11]. The current-voltage (I-V) characteristics of the real Schottky barrier diodes (SBDs) usually deviate from the ideal thermionic emission (TE) current transport model [4-9, 11-17]. Generally, the Schottky barrier height Φ_{b0} was found to decrease, while the ideality factor n increases, with decreasing temperature [8, 9, 11-17]. The increase in ideality factor with decreasing temperature is known as T_0 effect [18]. The decrease in barrier height at low temperatures leads to non-linearity in the plot of the activation energy $\ln(I_0/T^2)$ versus $1/T$.

Temperature-dependent characteristics of Schottky contacts in n-type InP has been reported by many researchers [19-22]. Cetin et al [19] studied temperature dependence of electrical characteristics of Au/InP Schottky barrier diode. They observed that the ideality factor decreases while the barrier height increases with increase of temperature. Cimilli et al [20] fabricated Au/n-InP/In Schottky barrier diodes, and reported that the barrier height varied from 0.557 eV to 0.615 eV and the ideality factor from 1.002 to 1.087. Recently, Ashok et al [21] studied the current-voltage-temperature (I-V-T) characteristics of Pd/n-InP Schottky diodes and found that the barrier parameters vary significantly with temperature. More recently, Cimilli et al [22] investigated the temperature-dependent electrical properties Ag/n-InP/In Schottky diodes in a wide temperature range (30 K to 320 K). In the present work, the I-V characteristics of Ru Schottky contacts on n-type InP substrate are measured in the temperature range of 200 – 400 K. The experimental

results show that the ideality factor, barrier height and series resistances are found to be strongly dependent on the temperature. The temperature dependent barrier characteristics of the Ru/n-InP Schottky contacts are interpreted on the basis of existence of Gaussian distribution of the barrier heights around a mean value due to barrier height inhomogeneities prevailing at the MS interface.

2. Experimental details

The samples used in this study are LEC grown undoped n-InP (100). The samples are initially degreased with organic solvents like trichloroethylene, acetone and methanol by means of ultrasonic agitation for 5 min in each step to remove contaminants followed by rinsing in deionized water and then dried in N₂ flow. The samples are then etched with HF (49%) and H₂O (1:10) to remove the native oxides from the substrate. Ohmic contacts of thickness 700 Å are formed on the rough side of the InP wafer prior to Schottky diode fabrication under a pressure of 7×10⁻⁶ mbar. The samples are then annealed at 350 °C for 1 min in N₂ atmosphere. Circular metal contacts, 1 mm in diameter and 500 Å thick, are deposited on the polished side of the InP wafer by evaporating Ru through a metal contact mask of 1 mm diameter. In order to reduce irradiation by stray electrons during evaporation, the InP material was screened from electrons originating at the filament of the electron beam evaporator [23]. The I-V characteristics were measured in the temperature range 200 – 400 K in steps of 40 K using SEMILAB DLS – 83D deep level spectrometer.

3. Results and discussion

3.1. Analysis of I-V characteristics of Ru/n-InP as a function of temperature

The semi-logarithmic I-V characteristics of the Ru/n-InP (100) SBDs in the temperature range of 200-400 K in steps of 40 K are shown in Fig. 1. Current transport in Schottky contacts is due to majority carriers and it may be described by thermionic emission over the interface barrier [6]. From thermionic emission theory, the current – voltage (I-V) relationship for Schottky barrier diode is given by the expression [6,7].

$$I = I_0 \exp\left(\frac{qV}{nkT}\right) \left[1 - \exp\left(\frac{-qV}{kT}\right) \right] \quad (1)$$

Where V is the applied voltage drop across the junction barrier, q is the electronic charge, k is Boltzmann's constant, T the absolute temperature in Kelvin, n the diode ideality factor and I₀ is the saturation current. I₀ is derived from the straight line intercept of ln[I/(exp(-qV/kT))] versus V at V=0, is expressed [2,6,9,10] as

$$I_0 = AA^{**} T^2 \exp\left(\frac{-q\Phi_{b0}}{kT}\right) \quad (2)$$

where A is the diode area, A^{**} is the effective Richardson constant equals to 9.4 Acm⁻² K⁻² based on effective mass (m* = 0.078m₀) of n-InP and Φ_{b0} is the apparent barrier height. The reverse saturation current I₀ decreased sharply with the decrease of the temperature as can be seen from Fig. 1.

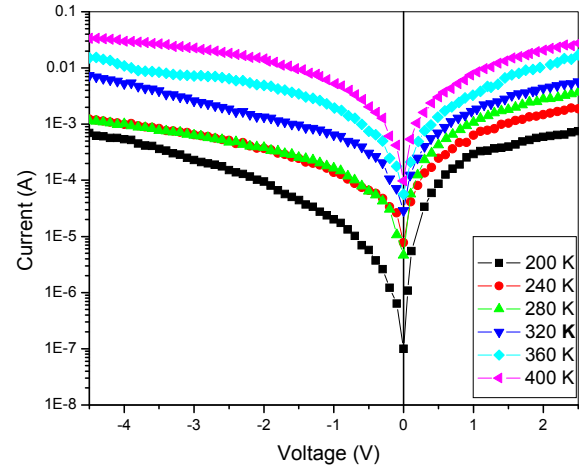


Fig. 1. I-V Characteristics of Ru contacts of Ru/n-InP Schottky barrier diode in the temperature range of 200 - 400 K.

A plot of I/[1-exp(-qV/nkT)] versus V, shown in Fig. 2 yields I₀ as the intercept. Once I₀ is determined, the barrier height (Φ_{b0}) can be evaluated using

$$\Phi_{b0} = \frac{kT}{q} \ln\left(\frac{AA^{**} T^2}{I_0}\right) \quad (3)$$

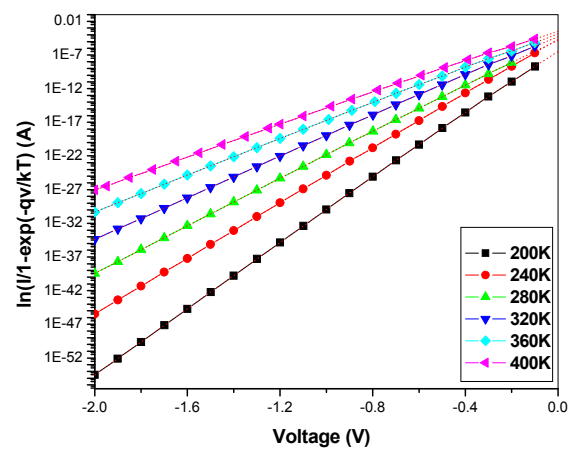


Fig.2. Plot of I/[1-exp(-qV/kT)] versus V for Ru/n-InP Schottky contacts as a function of temperature.

The ideality factor n is a measure of conformity of the diode to pure thermionic emission and is determined from the slope of the linear region of the plot of natural log of forward current versus forward bias voltage and is given by

$$n = \frac{q}{kT} \left(\frac{dV}{d(\ln I)} \right) \quad (4)$$

$n = 1$ for an ideal diode. Nevertheless, ideality factor n has usually a value greater than unity. Calculations using Eqs. (3) and (4) showed that the values of the apparent barrier height and ideality factor have changed from 0.39 eV and 4.2 at 200 K to 0.60 eV and 2.5 at 400 K respectively. The values for the barrier height are effective values and do not take into account image force lowering.

The values of the ideality factor n and barrier height Φ_{b0} of the diode at different temperatures are plotted as a function of temperature in Fig.3. The barrier height Φ_{b0} and ideality factor n are found to be a strong function of temperature. The plot shows that the ideality factor n exhibits an increasing trend with decreasing temperature, whereas the zero-bias barrier height Φ_{b0} shows decreasing trend as temperature decreases. Since current transport across the MS interface is a temperature activated process, electrons at low temperatures are able to surmount the lower barriers and therefore, current transport will be dominated by current flowing through the patches of lower SBH and a larger ideality factor. As temperature increases, more and more electrons have sufficient energy to surmount the higher barrier. As a result, both $\Phi_{b0}(I-V)$ and n are strongly dependent on temperature.

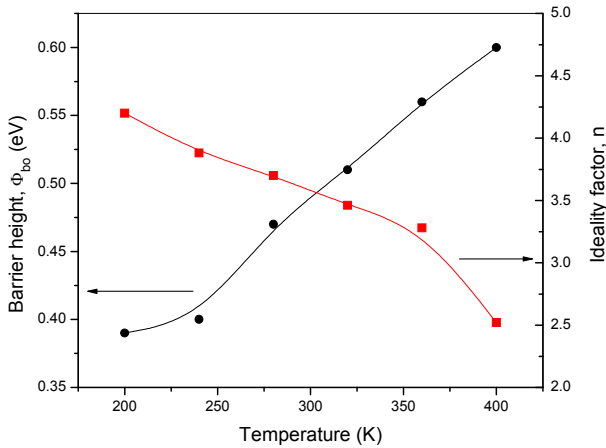


Fig.3. Temperature dependence of the ideality factor and zero-bias apparent height for Ru/n-InP Schottky barrier diode in the temperature range 200 – 400K.

The large values of the ideality factor show that there is a deviation from TE theory for current mechanism. It can be attributed to the presence of the interfacial thin native oxide layer between the metal and semiconductor [24]. Only the barrier inhomogeneities are very important for explaining the higher values of the ideality factor. The

variation of ideality factor with temperature is shown in Fig. 3. As shown the ideality factors n are not constant with temperature. Such behaviors of the diode ideality factor have been attributed to particular distribution of surface states [25]. The ideality factor of the diodes varies with temperature as

$$n(T) = n_0 + \frac{T_0}{T} \quad (5)$$

where n_0 and T_0 are constants which were found to be 1.50 and 566 K respectively. The increase in ideality factor with decreasing temperature as shown in Fig. 4 is known as T_0 effect. Explanations of the possible origin of such cases have been proposed taking into account the interface state density distribution, quantum mechanical tunneling and image force lowering [7].

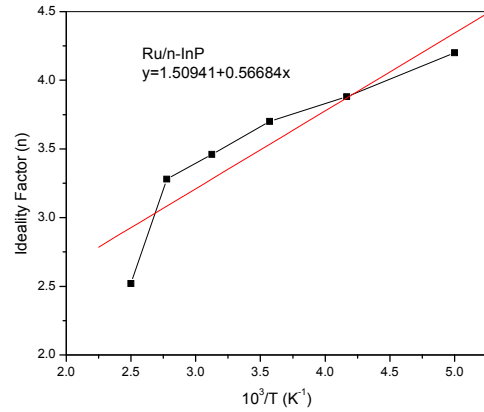


Fig.4. Temperature dependence of the ideality factor for Ru/n-InP Schottky barrier diode in the temperature range 200 – 400K.

3.2. Flat-band barrier height

The barrier height, which decreases with decreasing temperature obtained from Eq. (3) is called apparent or zero-bias barrier height. The barrier height obtained under flat-band condition is called flat-band barrier height and is considered to be real fundamental quantity. Unlike the case of the zero-bias barrier height, the electric field in the semiconductor is zero under the flat-band condition. This eliminates the effect of tunneling and image force lowering that would affect the I-V characteristics and removes the influence of lateral inhomogeneity [14,26]. To find the value of Φ_{bf} , the following expression is used [27,28]:

$$\Phi_{bf} = n\Phi_{b0} - (n-1) \left(\frac{kT}{q} \right) \ln \left(\frac{N_C}{N_D} \right) \quad (6)$$

where N_C is the effective density of states in the conduction band and N_D the carrier concentration. Fig. 5 shows the variation of flat-band barrier height Φ_{bf} as a

function of the temperature. Φ_{bf} is always larger than zero-bias barrier height Φ_{b0} and appears at first glance to be nearly constant with a slight variation. However, Φ_{bf} is obtained to increase with decreasing temperature in a manner similar to those reported by the others [26-30]. Furthermore, the temperature dependence of the flat-band barrier height can be expressed as

$$\Phi_{bf}(T) = \Phi_{bf}(T=0) + \alpha T \quad (7)$$

where $\Phi_{bf}(T=0)$ is the zero-temperature flat-band barrier height and α is the temperature coefficient of Φ_{bf} . In Fig. 5, the fitting of $\Phi_{bf}(T)$ data in Eq. (7) yields $\Phi_{bf}(T=0) = 1.04$ eV and $\alpha = -18.1$ meVK⁻¹.

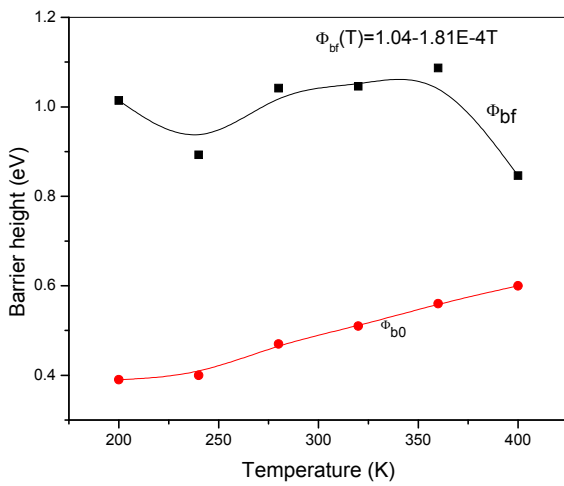


Fig. 5. Temperature dependence of the zero-bias barrier height, flat-band barrier height for the Ru/n-InP Schottky barrier diode. The circles represent Φ_{b0} and squares represent Φ_{bf} .

Where N_C and N_D are respectively the effective density of states in the conduction band and the donor density. N_C is defined as $2(2\pi m^* kT/h^2)^{3/2}$ with m^* being the majority carrier effective mass, $m^* = 0.077 m_e$ for n-InP [3]. Assuming the effective mass m^* and donor concentration N_D do not change with temperature, then the effective density of states N_C will change with temperature according to the relation

$$N_C \text{ (cm}^{-3}\text{)} = 1.8519 \times 10^{17} (T)^{3/2} \text{ cm}^{-3} \quad (8)$$

The temperature dependent N_C and N_D values are used in calculating Φ_{bf} values. The values of N_C are 5.2379×10^{20} cm⁻³ at 200K to 14.8152×10^{20} cm⁻³ at 400K, respectively.

3.3. Temperature dependent series resistance

Temperature dependency and the series resistance effect on the I-V characteristics of the Ru/n-InP Schottky diodes were investigated in the range 200-400 K. The resistance of the Schottky diode is the sum of the total resistance value of the resistors in series and resistance in semiconductor device in the direction of current flow. The series resistances were evaluated from the forward bias I-V data using the method developed by Cheung [31]. The forward bias current-voltage characteristics due to thermionic emission of a Schottky contact with the series resistance can be expressed by Cheung's function [6, 7, 32]:

$$\frac{dV}{d(\ln I)} = IR_s + n \left(\frac{kT}{q} \right) \quad (9)$$

Fig. 6 shows the plot of $dV/d(\ln I)$ versus I as a function of temperature. Eq. (9) should give straight line for the data of downward curvature region in the forward bias I-V characteristics. Thus the slope of the plot of $dV/d(\ln I)$ versus I gives R_s as the slope and $n(kT/q)$ as the y-axis intercept. The values of R_s obtained from the plots are given in Table.1.

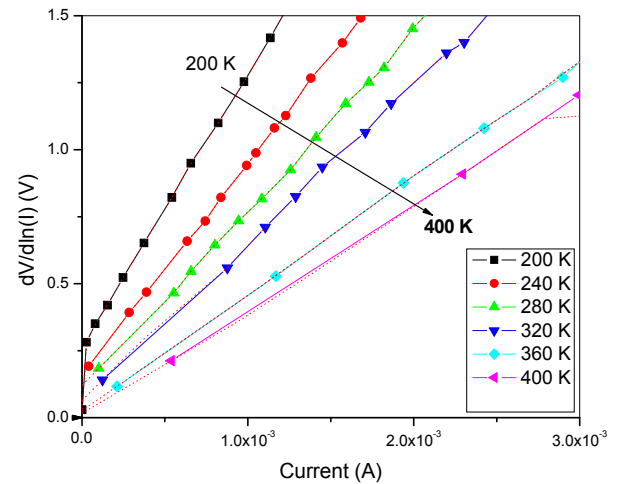


Fig. 6. Plot of $dV/d\ln(I)$ vs I for Ru/n-InP Schottky barrier diode.

Table 1. The experimentally obtained characteristic parameters of Ru/n-InP Schottky barrier diodes in the temperature range of 200 – 400K.

T(K)	Φ_{b0} (eV)	Φ_{bf} (eV)	n	R_s (Ω)
200	0.39	1.014	4.2	1070
240	0.40	0.893	3.8	798.22
280	0.47	1.042	3.7	392.43
320	0.51	1.046	3.4	253.12
360	0.56	1.087	3.2	38.31
400	0.60	0.846	2.5	31.56

Fig. 7 shows the experimental series resistance values from forward bias I-V characteristics as a function of temperature. The series resistance R_s obtained for each temperature using (Eq. (9)) of the I-V data is increasing with decrease of temperature. The increase of R_s with the fall of temperature is believed to be due to factors responsible for increase of n_{IV} and lack of free carrier concentration at low temperatures [5].

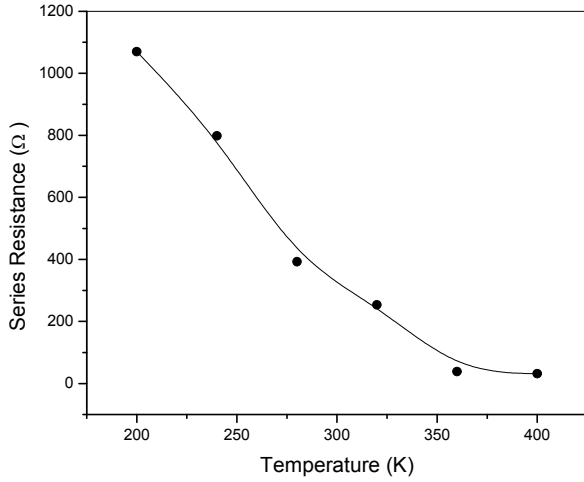


Fig.7. Temperature dependence of series resistance of Ru/n-InP Schottky barrier diode in the temperature range of 200 – 400 K.

3.4. Richardson plot

The barrier height can be determined in another way by rewriting Eq. (2) as

$$\ln\left(\frac{I_0}{T^2}\right) = \ln(AA^{**}) - \frac{q\Phi_{b0}}{kT} \quad (10)$$

The Richardson constant is usually determined from the intercept of $\ln(I_0/T^2)$ versus $1000/T$ plot. Fig.8 shows the plot of $\ln(I_0/T^2)$ against $10^3/T$ or $10^3/nT$. The plot between $\ln(I_0/T^2)$ versus $1000/T$ is found to be non-linear in the temperature measured. However, the dependence of $\ln(I_0/T^2)$ versus $10^3/nT$ gives a straight line. The non-linearity of $\ln(I_0/T^2)$ versus $10^3/T$ is due to the temperature dependence of the barrier height and ideality factor. Similar results have also been reported by several authors [15,29,30,33]. The experimental data are shown to fit asymptotically with a straight line at higher temperatures only. An activation energy value of 0.61 eV is obtained from the slope of this straight line. The values of A^{**} obtained from the intercept of the straight line portion at the ordinate of the experimental $\ln(I_0/T^2)$ versus $1000/T$ and $\ln(I_0/T^2)$ versus $1000/nT$ plot in Fig.8 are equal to $5.4 \times 10^{-5} \text{ A K}^{-2} \text{ cm}^{-2}$ and $2.02 \times 10^{-2} \text{ A K}^{-2} \text{ cm}^{-2}$ respectively. The value of A^{**} for electrons in n-type InP is much lower than the theoretically calculated value ($9.4 \text{ A K}^{-2} \text{ cm}^{-2}$ for n-type InP). The deviation in the Richardson

plots may be due to the spatially inhomogeneous barrier heights and potential fluctuations at the metal-semiconductor interface that consist of low and high barrier areas [5,13-15,25,33-35]. That is the current through the diode will flow preferentially through the lower barriers in the potential distribution [5,13-15,25,33-35].

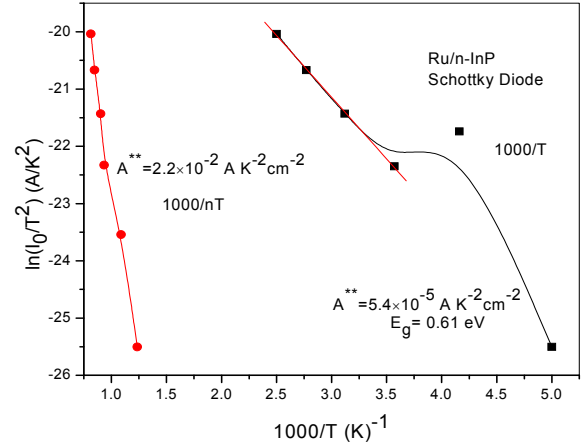


Fig.8. Richardson plots of $\ln(I_0/T^2)$ vs $10^3/T$ for Ru/n-InP Schottky diode.

3.5. Barrier height inhomogeneities

The ideality factor is simply a manifestation of the barrier uniformity and it increases for an inhomogeneous barrier [36]. An apparent increase in ideality factor and decrease in barrier height at low temperature are possibly caused by some other effects such as inhomogeneities of thickness and composition of the layer, non-uniformity of the interfacial charges or the presence of a thin insulating layer between the metal and the semiconductor [14,17,24,33,34]. Since current transport across the MS interface is a temperature-activated process, at low temperature, the current will be dominated by the current through the patches of low barrier height. Moreover, simulation studies of Freeouf et al [37] on mixed-phase Schottky contact reveal that, below a critical size, low barrier height region pinched off and only high barrier remains effective. Similar results obtained for the PtSi/Si diodes have been explained with an analytical potential fluctuation model for the interpretation of current-voltage and capacitance-voltage measurements on spatially inhomogeneous Schottky contacts proposed by Werner and Guttler [27,38]. According to Henisch [10], fluctuations in barrier heights are unavoidable, as they exist even in the most carefully fabricated systems.

Schmitsdorf et al [39] used Tung's theoretical approach and they found a linear correlation between the experimental zero-bias barrier height and the ideality factors. Fig. 9 shows a plot of the experimental SBH as a function of the ideality factor. As can be seen from Fig.9, there is a linear relationship between the experimentally effective barrier heights and the ideality factors of the Ru/n-InP Schottky barrier diodes that is explained by

lateral inhomogeneities of the BHs in the Schottky barrier diodes [39]. The extrapolation of the experimental Schottky barrier height versus ideality factor plot to $n=1$ has given a homogeneous barrier height of approximately 0.83 eV. The other barrier height values deviate from this value due to local inhomogeneities.

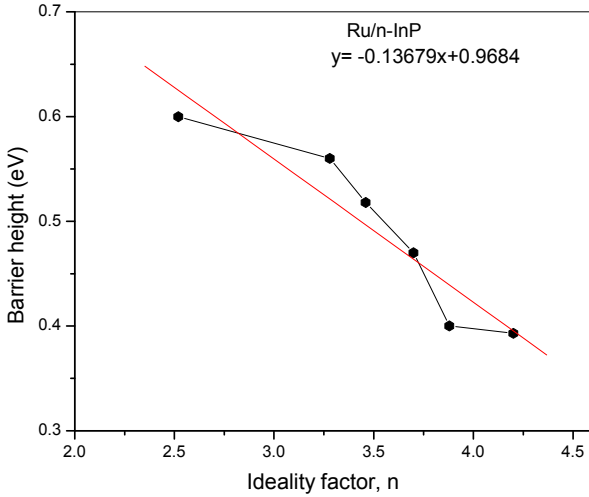


Fig.9. The zero-bias barrier height versus Ideality factor for the Ru/n-InP Schottky barrier diode.

In order to explain the abnormal behavior between the theoretical and experimental values of Richardson constants, let us assume that the distribution of the barrier heights has a Gaussian distribution with a mean values Φ_b and a standard deviation σ_s in the form of [34]:

$$P(\Phi_b) = \frac{1}{\sigma_s \sqrt{2\pi}} \exp \left[-\frac{(\Phi_b - \bar{\Phi}_b)^2}{2\sigma_s^2} \right] \quad (11)$$

The total current across the diode under the forward bias V is given by :

$$I(V) = \int_{-\infty}^{\infty} I(\Phi_b, V) P(\Phi_b) d\Phi_b \quad (12)$$

where $I(\Phi_b, V)$ is the current at a bias V for a barrier of Φ_b based on the thermionic emission model. Substituting equations (1) and (11) into equation (12), and performing the integration it becomes

$$I(V) = I_0 \exp \left(\frac{qV}{kTn_{ap}} \right) \left[1 - \exp \left(-\frac{qV}{kT} \right) \right] \quad (13)$$

with

$$I_0 = AA^{**} T^2 \exp \left(\frac{-q\Phi_{ap}}{kT} \right) \quad (14)$$

where Φ_{ap} and n_{ap} are the apparent barrier height and apparent ideality factor respectively and are given by:

$$\Phi_{ap} = \bar{\Phi}_{b0}(T=0) - \frac{q\sigma_0^2}{2kT} \quad (15)$$

$$\left(\frac{1}{n_{ap}} - 1 \right) = \rho_2 - \frac{q\rho_3}{2kT} \quad (16)$$

It is assumed that the mean SBH ($\bar{\Phi}_b$) and σ_0 are linearly bias dependent on Gaussian parameters such as $\Phi_b = \Phi_{b0} + \rho_2 V$ and $\sigma_s = \sigma_0 + \rho_3 V$ where ρ_2 and ρ_3 are the voltage coefficients which may depend on temperature and they quantify the voltage deformation of the barrier height distribution. The temperature dependence of σ_s is usually small and can be neglected.

Fitting of the experimental data in Eqs. (2) or (14) and in (4) gives Φ_{ap} and n_{ap} respectively which obeys Eqs. (15) and (16). Thus the plot of Φ_{ap} versus $1/T$ (Fig.10) is a straight line that gives $\Phi_{b0}(T=0)$ and σ_0 from the intercept and slope respectively. The values obtained for $\Phi_{b0}(T=0)$ and σ_0 (the zero-bias Standard deviation) are 0.79 eV and 0.122 eV respectively. Thus, the standard deviation is $\sim 15.3\%$ of the mean barrier height. As reported, the barrier inhomogeneities can occur as a result of inhomogeneities in the composition of the interfacial oxide layer, non-uniformity of interfacial charges and interfacial oxide layer thickness [27,34]. The σ_0 is a measure of the barrier homogeneity. The lower value of σ_0 corresponds to a more homogeneous barrier height. It is observed that the value of $\sigma_0 = 0.122$ eV is not small compared to the mean value of $\Phi_{b0}(T=0) = 0.79$ eV and it indicates greater inhomogeneities at the interface. Nevertheless, this inhomogeneity and potential fluctuations dramatically affect low temperature I-V characteristics. It is responsible, in particular, for the curved behavior in the Richardson plot in Fig.10. [34]. Again, the plot of n_{ap} versus $1/T$ should be a straight line that gives voltage coefficients ρ_2 and ρ_3 from the intercept and slope respectively (Fig.10). The values of $\rho_2 = 0.533$ V and $\rho_3 = 0.0088$ V were obtained from the experimental n_{ap} versus $1/T$ plot. The linear behavior of this plot demonstrates that the ideality factor does indeed express the voltage deformation of the Gaussian distribution of the Schottky barrier height. Furthermore, the experimental results of n_{ap} fit very well with theoretical Eq.(16) with $\rho_2 = 0.533$ V and $\rho_3 = 0.0088$ V. The continuous solid line (squares) in Fig. 3. represents data estimated with these parameters using equation (16). Now, combining Eqs. (14) and (15), we get

$$\ln\left(\frac{I_0}{T^2}\right) - \left(\frac{q^2 \sigma_0^2}{2k^2 T^2}\right) = \ln(AA^{**}) - \frac{q\Phi_{b0}}{kT} \quad (17)$$

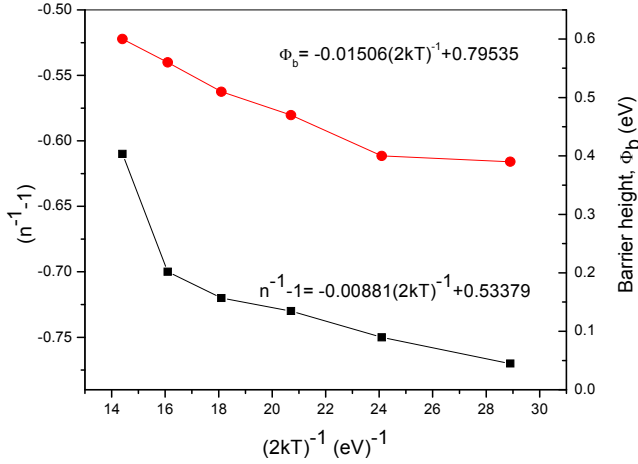


Fig.10. The zero-bias barrier height and Ideality factor vs $1/2kT$ curves of the Ru/n- InP Schottky barrier diode according to gaussian distribution of barrier heights.

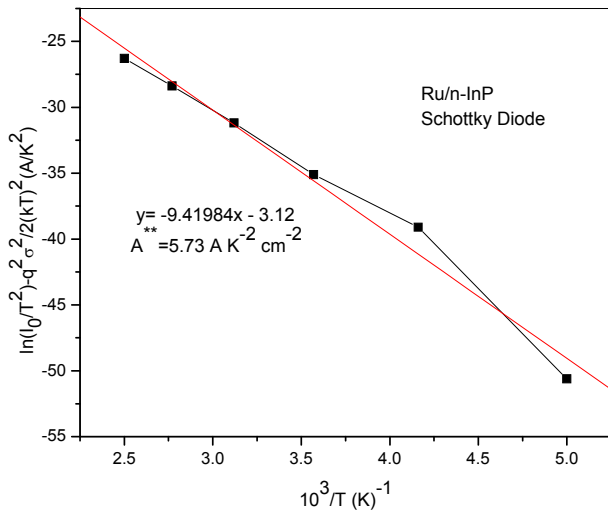


Fig. 11. Modified Richardson $\ln(I_0/T^2) - q^2 \sigma_0^2 / 2k^2 T^2$ vs $1/T$ plot for the device Ru/n-InP Schottky diode according to Gaussian distribution of the barrier heights.

A modified $\ln(I_0/T^2) - (q^2 \sigma_0^2 / 2k^2 T^2)$ versus $1/T$ plot according to Eq. (17) should give a straight line with the slope directly yielding the mean $\Phi_{b0}(T=0)$ and the intercept ($=\ln AA^{**}$) at the ordinate, determining A^{**} for a given diode area A . Fig.11 shows this plot. The modified $\ln(I_0/T^2) - (q^2 \sigma_0^2 / 2k^2 T^2)$ versus $1/T$ plot gives $\Phi_{b0}(T=0)$ and A^{**} as 0.81 eV and $5.73 \text{ A K}^{-2} \text{ cm}^{-2}$ respectively without using the temperature coefficient of the flat-band barrier height α . As can be seen, the value of $\Phi_{b0}(T=0) = 0.81 \text{ eV}$ from this plot is approximately

the same as the value of $\bar{\Phi}_{b0}(T=0) = 0.79 \text{ eV}$ from the plot of $\bar{\Phi}_{ap}$ versus $1/T$.

4. Conclusions

The current-voltage (I-V) characteristics of Ru/n-InP Schottky diodes were measured in the temperature rang 200 – 400 K. While the zero-bias barrier height Φ_{I-V} increased, ideality factor n and series resistance R_s decreased with increasing temperature. The changes are quite significant at low temperature due to the current transport can be controlled by the thermionic-field emission (TFE) theory. The origin and the nature of the increase in the ideality factor and decrease in the barrier height with decreasing temperature in the Ru/n-InP Schottky barrier diodes have been successfully explained on the basis of the thermionic emission with Gaussian distribution of the barrier heights $\Phi_{b0}(T=0) = 0.79 \text{ eV}$ and the S.D of 0.122 eV. The behavior is attributed to spatial inhomogeneities at the interface. The laterally homogeneous SBH value of approximately 0.83 eV for the Ru/n-InP (100) Schottky barrier diodes has been deduced from the linear relationship between the experimental barrier heights and ideality factors. The mean barrier height and the Richardson constant values were obtained as 0.81 eV and $5.73 \text{ A K}^{-2} \text{ cm}^{-2}$ respectively by means of the modified Richardson plot $\ln(I_0/T^2) - (q^2 \sigma_0^2 / 2k^2 T^2)$ versus $1/T$ which is in close agreement with the theoretical value of $9.4 \text{ A K}^{-2} \text{ cm}^{-2}$ for n- InP.

References

- [1] P. M. Smith, P. C. Chao, K. H. G. Duh, L. F. Lester B. R. Lee, Electron. Lett. **22**, 780 (1986).
- [2] C. W. Wilmsen, Physics and Chemistry of III – V Compound Semiconductor Interfaces, New York: Plenum, 1985.
- [3] K. Hattori, Y. Torii, Solid-State Electron. **34**, 527 (1991).
- [4] P. G. McCafferty, A. Sellai, P. Dawson, H. Elabd, Solid-State Electron. **39**, 583 (1996).
- [5] S. Chand, J. Kumar, Appl. Phys. A. **63**, 171 (1996).
- [6] E. H. Rhoderick, R.H. Williams, Metal-Semiconductor Contacts, Second ed., Clarendon press, Oxford, 1988.
- [7] S. M. Sze, Physics of Semiconductor Devices, Second ed., John Wiley and sons, New York, 1981.
- [8] E. Ayyildiz, A. Turut, H. Efeoglu, S. Tuzemen, M. Sagalam, Y. K. Yogurtcu, Solid-State Electron. **39**, 83 (1996).
- [9] R. T. Tung, Mater. Sci. Eng. R **35**, 1 (2001).
- [10] H. K. Henisch, Semiconductor Contacts, London: Oxford University, 123 (1984).
- [11] S. Chand, J. Kumar, Semicond. Sci. Technol. **10**, 1680 (1995).
- [12] S. Chand, Semicond. Sci. Technol. **17**, L36 (2002).

- [13] B. Abay, G. Cankaya, H. S. Guder, H. Efeoglu, Y. K. Yogurtcu, *Semicond. Sci. Technol.* **18**, 75 (2003).
- [14] A. Gumus, A. Turut, N. Yalcin, *J. Appl. Phys.* **91**, 245 (2002).
- [15] R. T. Tung, *Phys. Rev. B* **45**, 13509 (1992).
- [16] R. T. Tung, J. P. Sullivan, F. Schrey, *Mater. Sci. Eng. B* **14**, 266 (1992).
- [17] S. Karatas, S. Altindal, A. Turut, A. Ozmen, *Appl. Surf. Sci.* **217**, 250 (2003).
- [18] F. A. Padovani, G. Summer, *Appl. Phys. A* **36**, 3744 (1965).
- [19] H. Cetin, E. Ayyildiz, *Semicond. Sci. Technol.* **20**, 625 (2005).
- [20] F. E. Cimilli, M. Saglam, A. Turut, *Semicond. Sci. Technol.* **22**, 851 (2007).
- [21] A. Ashok Kumar, V. Janardhanam, V. Rajagopal, P. Narasimha Reddy, *J. Optoelectron. Adv. Mater.* **9**, 3877 (2007).
- [22] F. E. Cimilli, H. Efeoglu, M. Saglam, A. Turut, *J. Matter Sci: Mater. Electron.* (in Press).
- [23] G. Myburg, F. D. Auret, *J. Appl. Phys.* **71**, 6172 (1992).
- [24] S. Aydogan, M. Saglam, A. Turut, *Appl. Surf. Sci.* **250**, 43 (2005).
- [25] S. Zhu, R. L. Van Meirhaeghe, C. Detavernier, F. Cardon, G. P. Ru, X. P. Qu, B. Z. Li, *Solid-State Electron.* **44**, 663 (2000).
- [26] S. Hardikar, M. K. Hudait, P. Modak, S. B. Krupanidhi, N. Padha, *Appl. Phys. A* **68**, 9 (1999).
- [27] J. H. Werner, H. H. Guttler, *J. Appl. Phys.* **73**, 1315 (1993).
- [28] L. F. Wagner, R. W. Young, A. Sugerma, *IEEE Electron. Dev. Lett.* **4**, 320 (1983).
- [29] S. Chand, J. Kumar, *J. Appl. Phys.* **80**, 288 (1996).
- [30] F. E. Jones, C. D. Hafer, B. P. Wood, R. G. Danner, M. C. Lonergan, *J. Appl. Phys.* **90**, 1001 (2001).
- [31] S. K. Cheung, N. W. Cheung, *Appl. Phys. Lett.* **49**, 85 (1986).
- [32] A. Singh, *Solid-State Electron.* **28**, 223 (1985).
- [33] J. P. Sullivan, R. T. Tung, M. R. Pinto, W. R. Graham, *J. Appl. Phys.* **70**, 7403 (1991).
- [34] Y. P. Song, R. L. Van Meirhaeghe, W. H. Laflere, F. Cardon, *Solid-State Electron.* **29**, 633 (1986).
- [35] S. Chand, J. Kumar, *Semicond. Sci. Technol.* **11**, 1203 (1996).
- [36] S. Zhu, R. L. Van Meirhaeghe, S. Forment, G. P. Ru, X. P. Qu, B. Z. Li, *Solid-State Electron.* **48**, 1205 (2004).
- [37] J. L. Freeouf, T. N. Jackson, S. Laux, J. M. Woodall, *Appl. Phys. Lett.* **40**, 634 (1982).
- [38] J. H. Werner, H. H. Guttler, *J. Appl. Phys.* **69**, 1522 (1991).
- [39] R.F. Schmitsdorf, T.U. Kampen, W. Monch, *Surf. Sci.* **324** 249 (1995).

*Corresponding author: vjr.phd@gmail.com